International Journal of Earth Sciences
https://doi.org/10.1007/s00531-024-02408-8

ORIGINAL PAPER

Disparity between Toarcian Oceanic Anoxic Event and Toarcian carbon isotope excursion

Wolfgang Ruebsam[1] · **Lorenz Schwark**[1,2]

Received: 7 October 2023 / Accepted: 27 March 2024

Abstract

The Toarcian Oceanic Anoxic Event (T-OAE, Early Jurassic) is marked by widespread marine deoxygenation and deposition of organic carbon (OC)-rich strata. The genesis of the T-OAE is thought to be associated with environmental changes caused by the emission of ^{12}C-enriched greenhouse gasses (CO_2, CH_4), manifested in a negative Toarcian carbon isotope excursion (nT-CIE). The nT-CIE is commonly used to stratigraphically define the T-OAE, and despite the complex interrelationship of the different environmental phenomena, both terms (nT-CIE and T-OAE) are commonly used interchangeable. We here demonstrate that occurrence of OC-rich strata is diachronous and not restricted to the nT-CIE, reflecting the interaction of global- and regional-scale processes. Thus, the interchangeable use of T-OAE and nT-CIE should be discarded. The nT-CIE, however, hosts the T-OAE climax, marked by the widest extent of OC-rich strata. Early Toarcian environmental changes, particularly sea level rise and rising temperatures, may have made marine areas more susceptible to develop oxygen deficient conditions, favoring OC-accumulation.

Keywords Anoxia · Black shales · Carbon cycle · Carbon isotopes · Jurassic

Introduction

In the geological past, Earth's oceans were repeatedly punctuated by periods of severe deoxygenations, termed Oceanic Anoxic Events (OAEs), which in the geological record are manifested by the trans-regional-to-global scale occurrence of organic carbon (OC)-rich sedimentary rocks (black shales, sensu lato; Wignall 1994). Black shales are thought to have formed under oxygen deficient conditions (ODC) in marine settings (e.g., Schlanger and Jenkyns 1976; Tyson and Pearson 1991; Jenkyns 2010). OAEs occurred in conjunction with periods of environmental change and intense biogeochemical perturbations (e.g., Jenkyns 2010). In particular, global warming has been considered as major factor promoting deoxygenation in marine and lacustrine settings (e.g., Sarmiento et al. 1998; Keeling et al. 2010).

The early Toarcian stage (Early Jurassic, c. 183 Ma) records the Toarcian Oceanic Anoxic Event (T-OAE), characterized by the global-scale occurrence of OC-rich strata that formed on shelf seas, in deep marine settings and in (mega)lakes under ODC (e.g., Jenkyns and Clayton 1986; Jenkyns 1988; Littke et al. 1991a, b; Sundararaman et al. 1993; Röhl et al. 2001; Hermoso et al. 2013; Xu et al. 2017; Remírez and Algeo 2020; Kemp et al. 2022a, b). Global-scale increase in OC burial manifested in a long-lasting positive Toarcian carbon isotope excursion (pT-CIE) that spans most of the Toarcian *D. tenuicostatum* and *H. serpentinum* ammonite zone (or coeval chronozones) (Jenkyns and Clayton 1986; Jenkyns 1988; Jenkyns et al. 2001; Hougård et al. 2021). The pT-CIE is superimposed by the negative carbon isotope excursions at the Pliensbachian–Toarcian boundary (nP-T-CIE) and in the early Toarcian at the *D. tenuicostatum*–*H. serpentinum* zonal transition (nT-CIE), which have been recognized globally, making them robust chemostratigraphic markers (e.g., Fantasia et al. 2018; Ruebsam and Al-Husseini 2020; Al-Suwaidi et al. 2022; Kemp et al. 2022a). Negative carbon isotope anomalies reflect the release of large quantities of

✉ Wolfgang Ruebsam
wolfgang.ruebsam@ifg.uni-kiel.de

Lorenz Schwark
lorenz.schwark@ifg.uni-kiel.de

[1] Department of Organic and Isotope Geochemistry, Institute of Geoscience, University of Kiel, Kiel, Germany

[2] WA-OIGC, Curtin University, Perth, Australia

Published online: 05 May 2024

^{12}C-enriched greenhouse gases (CO_2, CH_4) into the Earth's ocean–atmosphere system that drove global warming (e.g., Hesselbo et al. 2000, 2007; Kemp et al. 2005; McElwain et al. 2005; Ruebsam et al. 2020a). Greenhouse gas emissions and global warming triggered a cascade of severe environmental changes, including intensified continental weathering (e.g., McArthur et al. 2000; Cohen et al. 2004; Percival et al. 2016; Them et al. 2017), glacio-eustatic sea level variations (Wignall 1991; Pittet et al. 2014; Krencker et al. 2019, 2022; Ruebsam et al. 2019, 2020b; Nordt et al. 2022), sluggish ocean circulation (Dera and Donnadieu 2012; Ruvalcaba Baroni et al. 2018; Fernández-Martínez et al. 2023) and freshening of some paleo-shelf seas (Sælen et al. 1996; Röhl et al. 2001; Dera and Donnadieu 2012; Remírez and Algeo 2020). Environmental changes are considered to be important factors causing marine oxygen depletion, which commonly initiates deposition of OC-rich sediments. Environmental perturbations may thus lead to stratigraphic correspondence between OC-rich sediments and the nT-CIE.

Accordingly, numerous works use the nT-CIE synonymous to the T-OAE, and due to the complex interrelationship of the different environmental phenomena, both terms (nT-CIE and T-OAE) are commonly used interchangeably. However, due to the complex interaction of global and local-scale oceanographic factors, such as water depth, nutrient supply, basin hydrology and water column stratification, the stratigraphic extent of OC-rich strata defining the T-OAE is not restricted to the nT-CIE, but shows a high spatial and temporal variability (e.g., Jenkyns and Clayton 1986; Jenkyns 1988; McArthur et al. 2008; Ruvalcaba Baroni et al. 2018; Fantasia et al. 2019a; Hougård et al. 2021). Consequently, the T-OAE, when defined based on the stratigraphic distribution of OC-rich sediments, varies greatly in its stratigraphic extent and thus in its duration.

Here, we discuss the spatio-temporal variability of early Toarcian OC-rich strata and redox conditions, as well as its stratigraphic relationship to the nT-CIE. Based on these data, the climax of the T-OAE can be defined as the stratigraphic interval in which the OC-rich deposits globally reach their greatest areal distribution. This interval is attributed to reflect the T-OAE (sensu stricto). The data further allow assessing global and local factors that controlled the development of ODC and the deposition of OC-rich sediments in marine and lacustrine settings.

Data and methods

Data compilation and synthesis

We compiled and synthesized OC abundances (OC = TOC, total organic carbon) and information on (qualitative) redox conditions from 48 lower Toarcian sections (Fig. 1). The data set includes previously and newly studied sites that preserve a presumably (near) complete record of the early Toarcian (Table S1 in the supplement). Sections without robust carbon isotope stratigraphy as well as sections with evidence for major hiatuses were excluded. Mean OC abundances were calculated and the redox regime was defined for globally correlative $\delta^{13}C$ segments (chemostratigraphic units: $\delta^{13}C$ falling limb, $\delta^{13}C$ rising limb, $\delta^{13}C$ valley, $\delta^{13}C$ plateau; see Ruebsam and Al-Husseini 2020). Therefore, the data summarize OC abundances and redox conditions for time intervals of about 0.4 Myr (e.g., Huang and Hesselbo 2014; Thibault et al. 2018; Ruebsam et al. 2023). Redox conditions were inferred from sedimentological and geochemical proxies. We here distinguish: i) oxic–dysoxic (O_2: >0.2 ml/lH_2O), ii) suboxic–anoxic (O_2: 0–0.2 ml/lH_2O), and

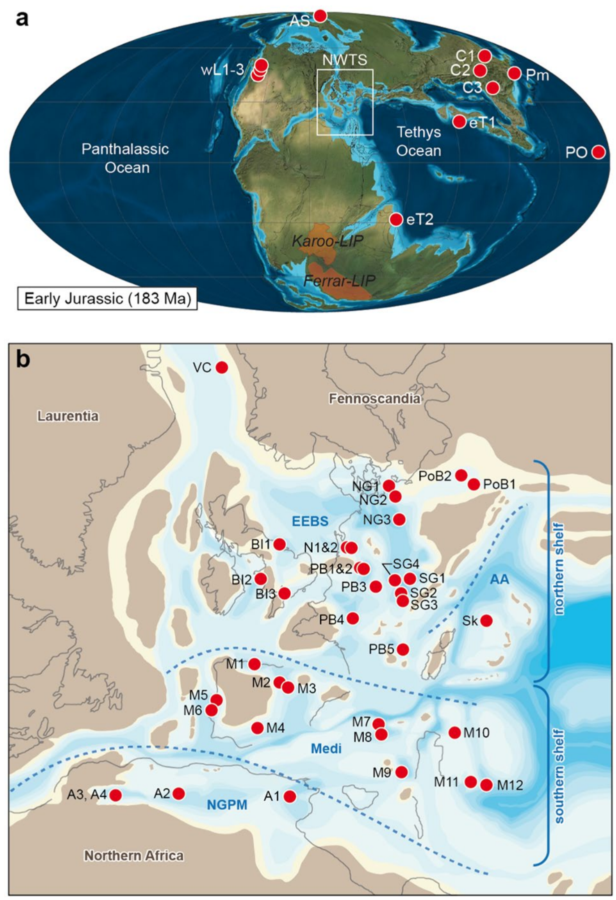

Fig. 1 **a** Global paleogeography during the Toarcian (Blakey 2016). **b** Paleogeography of the northwestern Tethys Shelf (NWTS) (Ruebsam et al. 2022a) showing the sites included in this study (AA: Austro-Alpine Sector; EEBS: European Epicontinental Basin System; Medi: Mediterranean Sector; NGPM: northern Gondwana Paleomargin). For abbreviations of the study sites were refer to Table S1 in the supplement (AS: Arctic Shelf; eT: East Tethys Ocean; Pm: Panthalassic Ocean margin; PO: Panthalassic Ocean; VC: Viking Corridor; wL: west Laurentia shelf)

iii) euxinic conditions (free H_2S) (see Tyson and Pearson 1991 and Fig. S1 in the supplement). Spatio-temporal patterns of sedimentary OC-enrichment and redox conditions were illustrated as matrix plots, generated using the PAST software toolkit (Hammer et al. 2001).

Results and discussion

Spatio-temporal distribution of early Toarcian organic carbon-rich strata

Our data synthesis reveals a substantial spatial and temporal variability of sedimentary OC abundances (mean abundances 0.1–15 wt.%) throughout upper Pliensbachian and lower Toarcian strata (Fig. 2; Table S1 in the supplement).

The most widespread occurrence of OC-rich strata with the highest OC contents is found in the northern NTWS area (Figs. 1, 2), a hydrogeographically restricted epicontinental basins system, with stagnant conditions and freshwater stratification (e.g., Sælen et al. 1996; Röhl et al. 2001; McArthur et al. 2008; Dickson et al. 2017; Ruvalcaba Baroni et al. 2018; Remírez and Algeo 2020; Fernández-Martínez et al. 2023). In this paleogeographic area, discrete OC-rich horizons were noted in some places at the Pliensbachian–Toarcian boundary and in the lower-middle part of the lower Toarcian *D. tenuicostatum* Zone ($\delta^{13}C$ plateau) (e.g., Röhl et al. 2001; Ruebsam et al. 2022a). However, substantial OC enrichment in sediments does not occur in most localities until the onset of the nT-CIE (e.g., Röhl et al. 2001; Hermoso et al. 2013; Ruebsam et al. 2022a; also see Table S1 in the supplement). At many localities of the northern NWTS, deposition of OC-rich sediments continued throughout the *H.*

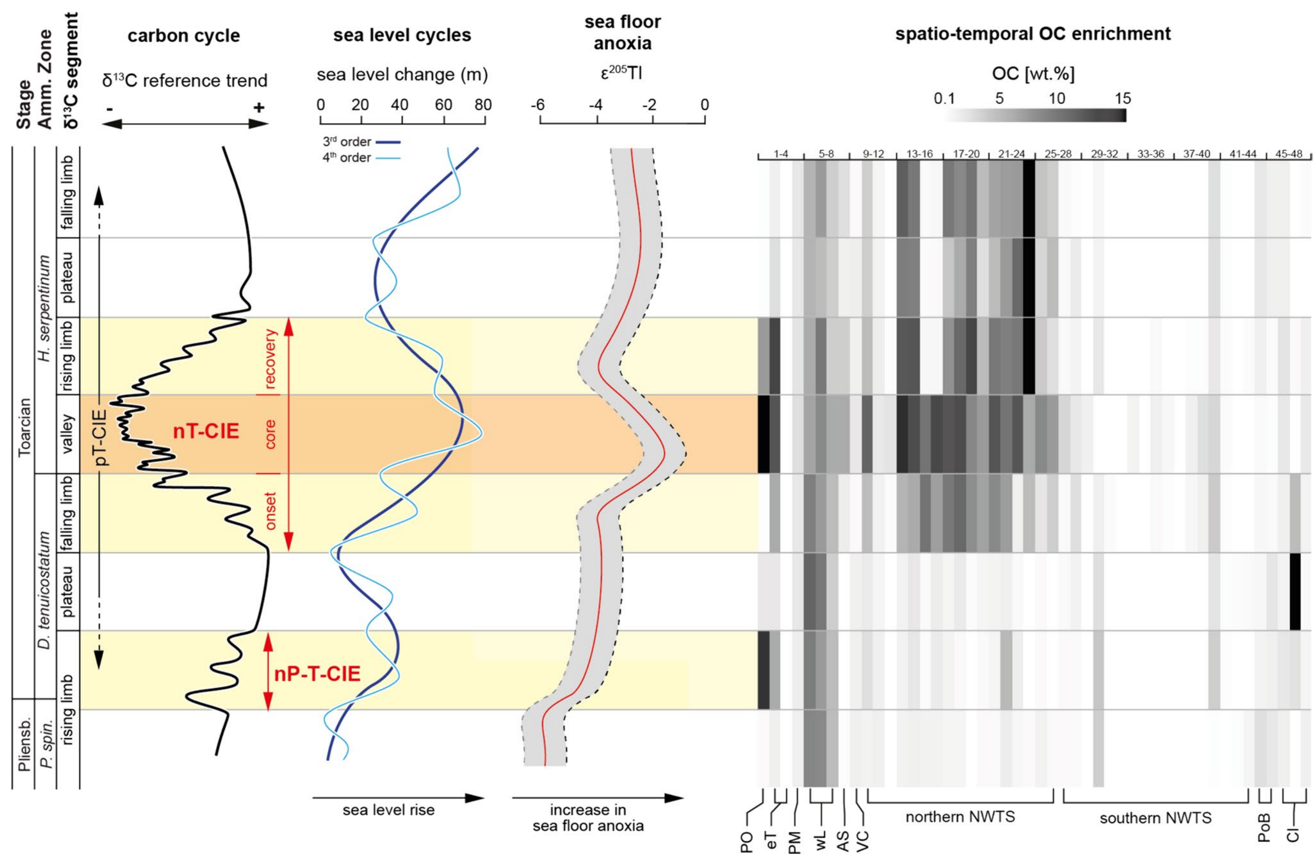

Fig. 2 Spatio-temporal enrichment of OC-rich strata. Stratigraphy of the early Toarcian, including ammonite zonation and carbon isotope stratigraphy (Ruebsam and Al-Husseini 2020). A positive carbon isotope excursion (pT-CIE) spans most of the early Toarcian and is intersected by negative carbon isotope excursions at the Pliensbachian/Toarcian boundary (nP-T-CIE) and in the early Toarcian (nT-CIE). Hypothetical sea level trend from Ruebsam et al. (2020b). Trends in thallium isotope values record changes of the extent in sea floor anoxia (Them et al. 2018). The matrix plot for mean OC abundance within a defined stratigraphic interval reveals a high spatio-temporal variability (NWTS: northwestern Tethys shelf; PO: Panthalassic Ocean, eT: East Tethys Ocean, PM: Panthalassic Ocean margin, wL: west Laurentia shelf; AS: Arctic Shelf, VC: Viking Corridor, PoB: Polish Basin, Cl: China (mega)lakes). Numbers at top of matrix plot indicate locations listed in Supplement 1

serpentinum Zone (e.g., Röhl et al. 2001; Hermoso et al. 2013) (Fig. 2). Exceptions are nearshore localities, such as the Grimmen Section (Prauss 1996), where OC-rich sediments are mostly confined to the nT-CIE onset and core intervals ($\delta^{13}C$ falling limb and valley).

A different pattern of the spatio-temporal OC accumulation is evident at sites in the Mediterranean sector of the southern NTWS (Fig. 1), a paleoceanographic area that was well connected to the Tethys Ocean (e.g., Dickson et al. 2017; Ruvalcaba Baroni et al. 2018; Fernández-Martínez et al. 2023). Here, mean OC values generally do not exceed 5 wt.%. Accumulation of OC occurs almost exclusively in sediments corresponding to the nT-CIE, with the highest OC concentrations documented in the nT-CIE core interval ($\delta^{13}C$ valley) (e.g., Jenkyns et al. 2001; Erba et al. 2022; also see Table S1 in the supplement). In addition, no significant OC enrichment occurred at many sites on the northern Gondwana paleomargin (southernmost NWTS, N-Africa) in upper Pliensbachian and lower Toarcian strata (e.g., Reolid et al. 2018) (Fig. 2). An exception is the area of present-day Tunisia, where OC-rich strata occur in the early Toarcian (Ruebsam et al. 2022b).

A similar pattern is observed on shelf areas in the eastern Tethys Ocean. In the Qiangtang Basin (NE Tethys margin), OC-rich strata occur at a local scale in the nT-CIE interval and in an interval potentially corresponding to the nP-T-CIE (e.g., Fu et al. 2017; Xia and Mansour 2022). Sediments of the Sewa Section in the Qiangtang Basin lack TOC-enrichment and evidence for OC accumulation (Fu et al. 2021), which point to spatial variations in depositional conditions within the basin. Sediments of the Niandua Section (SE Tethys margin) lack any OC-enrichment (Han et al. 2022) (Figs. 1, 2). In the deep marine Sakahogi Section (Panthalassic Ocean) substantial OC-enrichment (mean OC up to 15 wt.%) occurs in the nP-T-CIE interval (Kemp et al. 2022a) as well as in the nT-CIE core and recovery intervals ($\delta^{13}C$ valley and rising limb), whereas sediments of the other stratigraphic intervals are rather OC-lean (Fig. 2).

Sediments from the western Panthalassic margin (Sakuraguchi-dani, Japan; Izumi et al. 2018) exhibit no significant OC-enrichment. Early Toarcian sediments from the southeastern Panthalassic margin (Andean Basins) are also mainly TOC-lean (Fantasia et al. 2018). An exception is the Arroyo Lapa section (Neuquén Basin), were increased OC contents occur in an interval that may correspond to the nT-CIE onset (Al-Suwaidi et al. 2016). Sites from the West-Laurentia shelf (northeastern Panthalassic margin, N-America) show a substantial OC-enrichment throughout lower Toarcian times (Them et al. 2017, 2018), but also in upmost Pliensbachian strata (Fig. 2). Interestingly, OC contents peak at two sites just before the onset of nT-CIE, while OC content decreases within the nT-CIE interval (Fig. 2).

Site-specific patterns of OC accumulation have been documented in (mega)lakes in present-day China. In some (mega)lakes, abundances of aquatic OC decrease in the nT-CIE onset interval (Li et al. 2023) (Fig. 2). A decline in OC abundances in the nT-CIE interval was also documented for the Polish Basin. However, here OC abundances rather represent changes in the abundances in allochthonous land plant organic matter, which limits the comparability with coeval strata that is dominated by marine organic matter (Pienkowski et al. 2016).

Spatio-temporal redox pattern

As with OC abundances, there is considerable spatiotemporal variability in redox conditions. In the deep-marine Sakahogi Section (Panthalassic Ocean), a decline in seafloor oxygenation occurred at the Pliensbachian–Toarcian boundary and persisted into the nT-CIE recovery interval (Kemp et al. 2022a). The formation of euxinic bottom waters is indicated for the nP-T-CIE interval and the nT-CIE interval (Fig. 3; Table S1 in the supplement). Euxinic conditions also developed on the northern margin of the eastern Tethys Ocean, while the shelf seas on the southern margin remained oxygenated (e.g., Fu et al. 2017; Han et al. 2022). Preferentially oxic–dysoxic conditions are also indicated for the western margin of the Panthalassic Ocean (Japan) (Izumi et al. 2018), as well as from the southeastern margin of the Panthalassic Ocean (Andean Basins; Fantasia et al. 2018). In contrast, on the western Laurentia shelf (N America), anoxic–euxinic conditions predominated during the late Pliensbachian and early Toarcian (Them et al. 2018) (Fig. 3; Table S1 in the supplement). On the Arctic shelf, suboxic–anoxic conditions established in the nT-CIE onset interval and prevailed throughout the entire early Toarcian (Suan et al. 2011; Table S1 in the supplement).

On the northern NWTS, where black shale deposition was most extensive, anoxic–euxinic conditions became established over almost the entire area in the nT-CIE interval. In many localities, these conditions expanded into the *H. serpentinum* Zone (=*H. falciferum* Zone) (e.g., Littke et al. 1991a, b; Schouten et al. 2000; Schwark and Frimmel 2004; Reolid et al. 2018; Ruebsam et al. 2018; also see review by Kemp et al. 2022b and Table S1 in the supplement). At shoals and marginal sites, suboxic–anoxic conditions were restricted to the nT-CIE interval (see Table S1 in the supplement). Within the nT-CIE interval the onset of ODC was diachronous (Fig. 2). Some sites (e.g., Dotternhausen Section) record the development of ODC in the nT-CIE onset interval, while other sites (e.g., Sancerre Core) remained preferentially oxygenated until the nT-CIE core interval (Fig. S2 in the supplement). In the NE Paris Basin, anoxic–euxinic conditions are also indicated for the nP-T-CIE interval and for some horizons in the middle *D.*

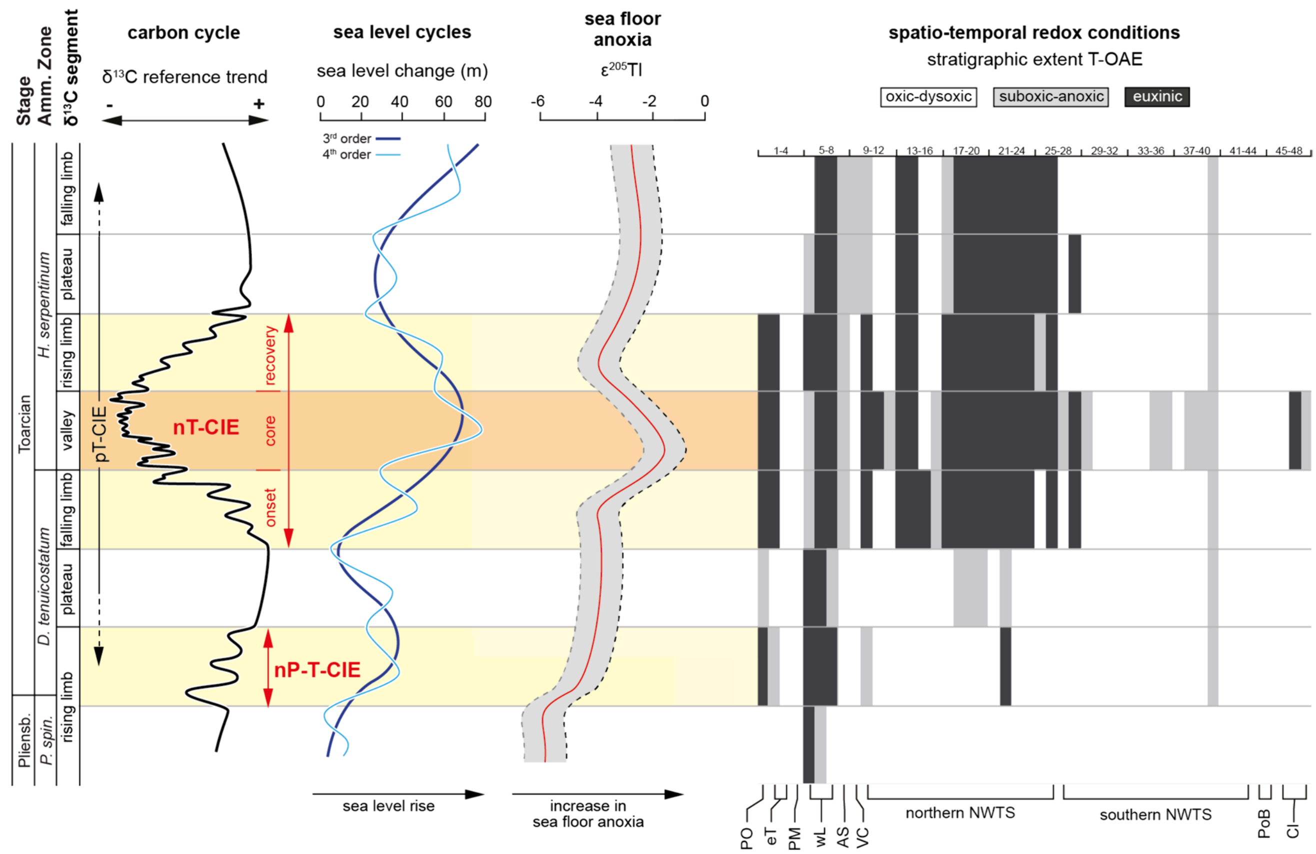

Fig. 3 Spatio-temporal redox pattern. The matrix plot illustrates spatio-temporal differences in the redox conditions for the different stratigraphic intervals in relation to trends in carbon isotopes, sea level and thallium isotopes (see Fig. 2 for abbreviations and details)

tenuicostatum Zone (δ^{13}C plateau). Evidence of short-lived anoxic–euxinic conditions in the middle *D. tenuicostatum* Zone also comes from the S-German Basin (Schwark and Frimmel 2004) (Fig. 3; Table S1 in the supplement).

At the southern NWTS, suboxic–anoxic conditions developed at some localities within the nT-CIE interval, especially in the nT-CIE core interval (δ^{13}C valley) (e.g., Jenkyns et al. 2001; also see Table S1 in the supplement). An exception is the Tunis Trough (N-Gondwana paleomargin), where suboxic–anoxic conditions prevailed in some graben structures throughout the early Toarcian (Ruebsam et al. 2022b) (Fig. 3; Table S1 in the supplement).

Marginal sites in the Polish Basin show no evidence for the development of ODC. Here, shallow water depths maintained an efficient ventilation of the sea floor (Pienkowski et al. 2016). Contrasting redox conditions were observed in the Chinese (mega)lakes (e.g., Liu et al. 2020; Huang et al. 2023a, b). Some lakes remained preferentially well-oxygenated, while others reveal evidence for suboxic–anoxic and euxinic conditions. However, if documented, ODC established in the nT-CIE core interval (Fig. 3; Table S1 in the supplement).

Controls on organic matter accumulation and redox conditions

The OC-richness and redox conditions reveal a comparable spatio-temporal pattern, confirming that the decline in O_2 levels at the shelf (and ocean) floor was an important factor promoting the preservation of labile aquatic organic matter and thereby the formation of OC-rich strata during the early Toarcian (e.g., Jenkyns 1988; Littke et al. 1991a, b; Röhl et al. 2001; Schwark and Frimmel 2004; Song et al. 2017; also see review by Kemp et al. 2022b; Fig. S3 in the supplement).

Initial increases in the mean OC content, the number of sites with OC-rich strata, and ODC occurred in the Pliensbachian/Toarcian boundary interval and were followed by a more pronounced propagation in the nT-CIE onset interval. Highest mean OC abundances, as well as the greatest extent of OC-rich strata and ODC occurred in the nT-CIE core interval (Fig. 4). Mean OC abundances, number of sites with OC-rich strata, and ODC remained high in the nT-CIE recovery and the post-nT-CIE intervals.

The stratigraphic pattern of OC enrichment and ODC matches trends in thallium isotope values, which are thought

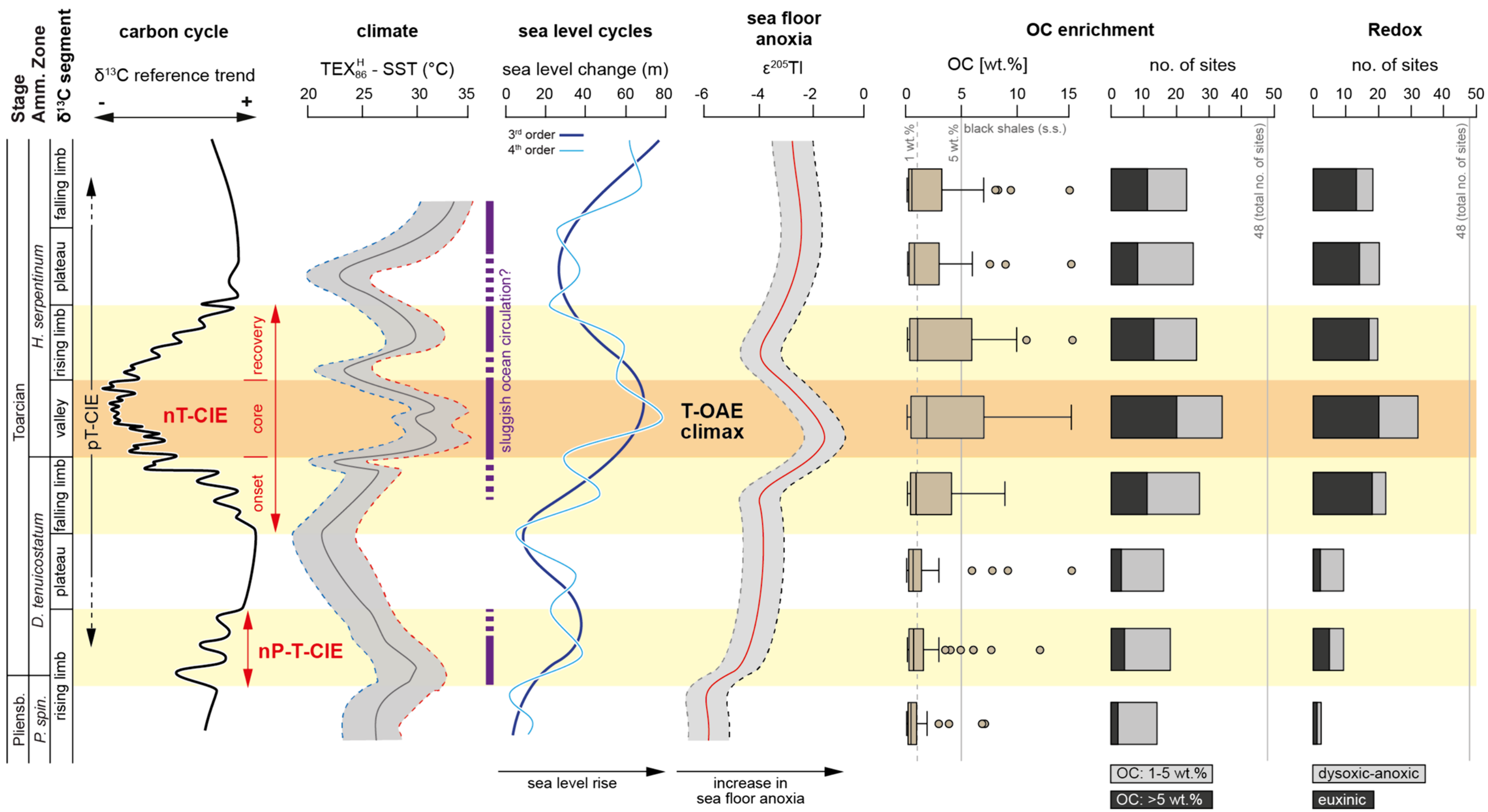

Fig. 4 Stratigraphic trends in carbon isotopes, sea-level and thallium isotopes together with mean OC abundances, the number of sites with OC enrichment and development of oxygen-deficient conditions within a defined stratigraphic interval. See text for discussion

to indicate the extent of anoxic sinks on a global scale (Them et al. 2018). The generalized trend in thallium isotope values records a shift towards heavier values in the Pliensbachian/Toarcian boundary interval, followed by a positive excursion in approximately the upper nT-CIE onset and the nT-CIE core intervals (Fig. 4). Interestingly, the nT-CIE onset and core intervals record evidence for (short-lived/periodic) euxinia even at a few sites with low to moderate OC accumulation (Fig. S3 in the supplement).

The pattern of declining seafloor oxygenation and OC-enrichments match transgressive pulses that occurred at the Pliensbachian/Toarcian boundary intervals as well as in the nT-CIE onset interval (e.g., Röhl et al. 2001; Hermoso et al. 2013; Pittet et al. 2014; Haq 2018; Krencker et al. 2019; Ruebsam et al. 2019, 2020b; Bodin et al. 2023). Most significantly, the major sea level rise that occurred in the early Toarcian, within the nT-CIE onset interval (e.g., Röhl et al. 2001; Krencker et al. 2019; Ruebsam et al. 2019), aligns with the strongest spread of OC enrichment and ODC (Fig. 4). Accordingly, a high sea level was a pre-requirement for maintaining ODC and OC-accumulation at shelf settings (e.g., Wignall 1991; Röhl et al. 2001; Hermoso et al. 2013). An overall high sea level may have also promoted ODC and OC-accumulation at the northern NWTS throughout the *H. serpentinum Zone* (approx. equal to the *H. falciferum* Zone) (e.g., Röhl et al. 2001; Hermoso et al. 2013). A high sea level resulted in flooding of large shelf areas with water depths, where the seafloor was below storm wave base. Here, low-energy depositional spaces formed (e.g., Wignall 1994). On the northern NWTS, where OC accumulation was most extensive, development of ODC was further promoted by freshwater stratification and severe hydrological restriction (Sælen et al. 1996; Röhl et al. 2001; McArthur et al. 2008; Dickson et al. 2017; Remírez and Algeo 2020; Fernández-Martínez et al. 2023). Freshwater stratification and hydrologic constraints may have weakened in the post nT-CIE period (upper *H. serpentinum* Zone and coeval strata), but were still sufficient to maintain ODC in bottom waters as long as the sea level was sufficiently high and the seafloor was no ventilated by wave and storm activity (e.g., McArthur et al. 2008). Accordingly, at the northern NWTS, long-lasting ODC and OC accumulation resulted from the very specific paleogeographic and hydrogeographical of this highly restricted shelf sea. Moreover, the area of the northern NWTS was situated in a humid climate belt with high precipitation rates and substantial riverine runoff (e.g., Rees et al. 2000; Dera et al. 2009; Ruebsam et al. 2020c). Riverine freshwater supply, in addition to freshwater inflow from the Arctic Ocean via the Viking Corridor (Sælen et al. 1996; Bjerrum et al. 2001), contributed to stratification of the water column in this highly restricted shelf setting. In addition, riverine freshwater runoff will have contributed huge amounts of nutrients to the shelf sea and thereby stimulated and maintained marine primary productivity. Globally increased temperatures and increased precipitation at mid-latitudes were initiated during the nT-CIE but persisted throughout most of the Toarcian (Dera et al. 2009, 2011). Accordingly, at the northern NWTS, black shale deposition was not restricted to the nT-CIE interval. Differences in the stratigraphic extent of OC-rich strata most likely reflect paleobathymetry, with black shales being most extensive at deep settings, being of short stratigraphic extent or even being absent at shallow settings.

At the southern part of the NWTS, the lack of hydrological restriction, more arid conditions and low-to-moderate riverine runoff did not favor the development of freshwater stratification. At this shelf area, water column stratification (if present) may have resulted from thermal stratification. However, marine primary productivity appears to have been insufficiently high to cause prolonged ODC and substantial OC accumulation (Ruebsam et al. 2020d; Baghli et al. 2022). At the southern NWTS, OC-rich strata has been reported from some deep marine settings, such as in the Belluno Trough (Jenkyns et al. 2001; Dickson et al. 2017) and the Lombardian Basin (Erba et al. 2022). At these settings sea-level variation will have had no impact on depositional conditions. However, sluggish ocean circulation, related to changes in global climate conditions may have led to a decline in seafloor O_2 levels and to the accumulation of OC-rich strata (Dera and Donnadieu 2012; Ruvalcaba Baroni et al. 2018). Sluggish ocean circulation could have been particularly pronounced during periods of globally high temperatures, reduced sea ice cover, and lack of continental glaciation (Dera and Donnadieu 2012) (Fig. 4). Such conditions were most likely realized during the Pliensbachian/Toarcian boundary and in the nT-CIE core interval that both record thermal maxima in sea surface temperatures and coinciding (glacio)eustatic sea level rises (Krencker et al. 2019; Ruebsam et al. 2019, 2020a, b; Nordt et al. 2022). The occurrence of OC-rich anoxic/euxinic strata in deep oceanic areas substantiates such a scenario (Kemp et al. 2022a).

Prolonged ODC and OC-accumulation occurring throughout the entire early Toarcian on the west Laurentia shelf could be explained by local factors, such as upwelling long the eastern Panthalassic margin that may have stimulated marine primary productivity (Parrish and Curtis 1982). The declining trend in OC accumulation and ODC, noted at some sites from the western Laurentia shelf, might be partly linked to reduced upwelling that occurred in response to sluggish ocean circulation. Alternatively, increased supply of clastics from continental areas during periods of enhanced weathering may have also led to the decline in the sedimentary OC-content (Them et al. 2017).

Defining the T-OAE

The spatio-temporal variability of Toarcian OC-rich sediments and ODC shows that neither OC richness nor redox state are suitable parameters to precisely define a distinct (chrono)stratigraphic event or interval. The deposition of OC-rich strata occurred in response to global driving forces interacting with local-to-regional-scale factors. Accordingly, onset, termination and thus stratigraphic extent of OC-rich strata varied substantially. In addition, OC-rich sediments and the formation of ODC were not restricted to the nT-CIE interval, which is frequently used to define the T-OAE (e.g., Hesselbo et al. 2007; Fantasia et al. 2018, 2019a; Danise et al. 2019; Visentin et al. 2021; Galasso et al. 2022; Trabucho-Alexandre et al. 2022).

The nT-CIE onset (δ^{13}C falling limb) interval, however, records the diachronous onset of ODC and OC accumulation in a great number of marine regions, as well as substantial increase in mean sedimentary OC content. The widest areal extent of OC-rich strata and ODC, together with highest mean OC contents is seen in the nT-CIE core interval (δ^{13}C valley). This observation gives some justification to the approach of equalizing the T-OAE with the nT-CIE.

The nT-CIE interval, in particular the onset and core intervals, corresponds to a period of severe environmental and ecosystem change, summarized by the term "Jenkyns Event" (Müller et al. 2017; Reolid et al. 2021). This period may mark a tipping point in the Earth's climate system that once crossed, made marine (and lacustrine) depositional systems more susceptible for the development of ODC.

In general, distinct OC-enrichment and redox pattern can be distinguished and can be linked to specific depositional settings (Fig. 5). Open deep marine (unrestricted) as well as oceanic settings record a diachronous T-OAE within the nT-CIE interval (T-OAE—type 1). Restricted shelves, such as the northern NWTS, exhibit prolonged ODC and OC accumulation with diachronous onset in the nT-CIE interval, but in many localities significantly exceed this interval (T-OAE—type 2). Along upwelling regions of the western Laurentia shelf (NE Panthalassic Ocean), ODC and OC-accumulation persisted throughout the entire early Toarcian and thus pre- and post-date the nT-CIE. In these settings, the T-OAE is decoupled from the nT-CIE (T-OAE—type 3a) (Fig. 5). One could argue that such a pattern of prolonged anoxia and OC accumulation indicates an anoxic episode rather than an anoxic event (sensu stricto).

In the lacustrine Ordos Basin (Chinese), where the accumulation of (aquatic) OC peaked before the nT-CIE and declined in this interval (Jin et al. 2020), ODC appear to have developed primarily in the nT-CIE interval (Huang et al. 2023a, b). Accordingly, ODC were not the major factor controlling OC-accumulation in this setting. However, in most Toarcian mega-lakes that have been studied so far, evidence for ODC and OC accumulation is restricted to the nT-CIE interval (e.g., Xu et al. 2017; Huang et al. 2023a, b; also see Table S1 in the supplement).

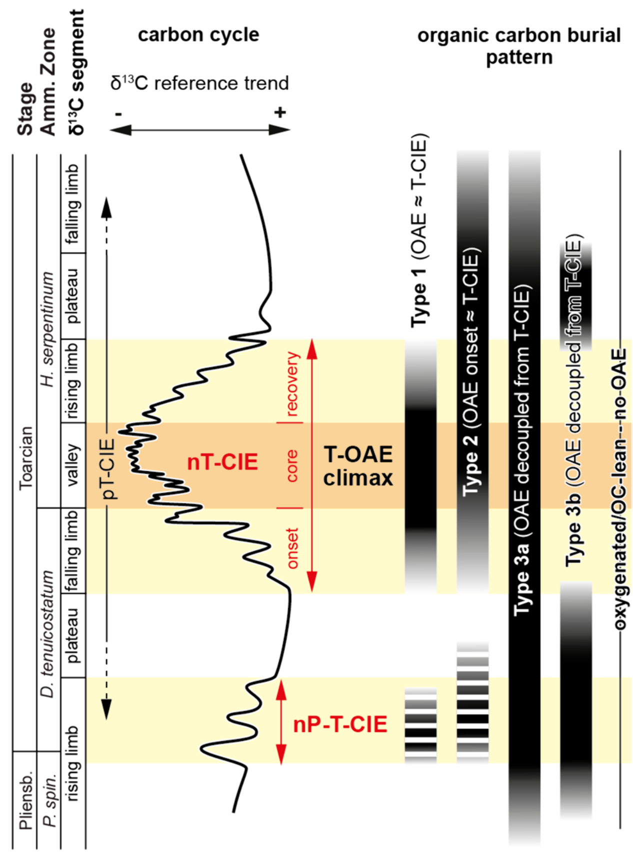

Fig. 5 T-OAE, when defined as OC burial event, exhibits a substantial spatio-temporal variability, whereby three main types (stratigraphic patterns) can be distinguished. Type 1 is mainly documented from oceanic and open (unrestricted) shelf seas. Type 2 is characteristic for the T-OAE on the northern NWTS, where deposition of OC-rich strata was most widespread. Locally, OC-rich strata can also occur in the form of distinct horizons at the Pliensbachian–Toarcian boundary and in the lower part of the *D. tenuicostatum* Zone. A stratigraphically extended T-OAE of the Type 3a is documented from the western Laurentia shelf. T-OAEs of type 3b are noted in a very few sites only and may reflect local-scale depositional conditions. It is particularly important that the OAEs of type 3a and 3b are decoupled from the nT-CIE. Numerous early Toarcian sections lack evidence of ODC and OC-accumulation. For such settings, the term OAE is inappropriate and should be avoided

In the Sierra Palomera Section (Spain), ODC and OC-accumulation peak in strata pre- and posting dating the nT-CIE, while the nT-CIE interval is represented by OC-lean strata (Danise et al. 2019). The development of an OAE prior and/or after the nT-CIE may categorize a T-OAE—type 3b, which most likely reflects local depositional conditions.

The high spatio-temporal variability complicates the exact definition of a T-OAE, in terms of a global marine deoxygenation event. The climax of the T-OAE, however, can be placed in the nT-CIE core interval, showing the highest mean OC abundances, as well as the widest extent of OC-rich strata and ODC. This interval further correlates with the positive thallium isotope peak that reflects the widest extent of marine anoxic sinks (Them et al. 2018). We, therefore, attribute the nT-CIE core interval to the T-OAE climax, which defines the stratigraphic interval that records the widest extent of OC-accumulation and ODC (Figs. 4, 5). Climate-enforced changes in environmental condition occurring in the nT-CIE interval and to a lesser extent in the Pliensbachian–Toarcian boundary interval may have made marine and lacustrine environments more susceptible to ODC, which favored the preservation and accumulation of OC-rich strata.

During the early Toarcian, numerous sites in different paleogeographic areas lack evidence for ODC and OC accumulation, such as most sites at the northern Gondwana paleomargin (e.g., Bodin et al. 2010; Krencker et al. 2019, 2022), in Spain (Reolid et al. 2018; Silva et al. 2021), in Portugal (Hesselbo et al. 2007; Fantasia et al. 2019a), in Italy (Fantasia et al. 2019b), or in southern America (Fantasia et al. 2018). At these settings no OAE developed in the early Toarcian. Accordingly, the stratigraphic interval that records the nT-CIE should not be assigned as T-OAE. Early Toarcian sites that record no OAE should rather be attributed to the Jenkyns Event, as previously suggested by Müller et al. (2017) and Reolid et al. (2021).

Conclusions

The early Toarcian records the global-scale occurrence of OC-rich strata that has been deposited under ODC (suboxic/anoxic to euxinic conditions) during the T-OAE. Both parameters, OC-richness and redox conditions, however, revealed a substantial spatio-temporal variability, resulting from the interaction of global forcing mechanisms (e.g., climate, ocean circulation, eustatic sea level) and local basin-scale factors (e.g., basin morphology, hydrologic restriction, water column stratification, nutrient supply). Therefore, onset and termination of OC accumulation and ODC was evidently diachronous and varied at basin to sub-basin scale. Accordingly, OC richness and ODC are inadequate parameters for defining a distinct (chrono)stratigraphic event, such as the T-OAE.

Moreover, OC-rich strata are not restricted to the nT-CIE. Thus the interchangeable use of T-OAE and nT-CIE (commonly: T-CIE), as applied by numerous works, is misleading and should be discarded. An initial increase in global OC-accumulation occurred in the Pliensbachian–Toarcian boundary interval, while a substantial spread in OC-rich strata occurred in the nT-CIE onset interval. Accumulation of OC-rich strata and ODC, as well as highest mean OC contents are documented in the nT-CIE core interval, marking the T-OAE climax. Data indicate that early Toarcian environmental changes turned marine (and lacustrine) environments more susceptible to ODC, favoring the preservation and accumulation of OC-rich strata.

Supplementary Information The online version contains supplementary material available at https://doi.org/10.1007/s00531-024-02408-8.

Acknowledgements The authors declare that they have no known competing financial interests or personal relationships that could have appeared to influence the work reported in this paper. Financial support of this project by the German Research Foundation (DFG grant Schw554-29) is gratefully acknowledged. The constructive comments by Javier Fernández-Martínez and an anonymous reviewer are highly appreciated.

Funding Open Access funding enabled and organized by Projekt DEAL.

Data availability Data are provided as supplementary table (supplementary file 1).

References

Al-Suwaidi AH, Hesselbo SP, Damborenea SE, Mancenido MO, Jenkyns HC, Riccardi AC, Angelozzi GN, Baudin F (2016) The Toarcian Oceanic Anoxic Event (Early Jurassic) in the Neuquén Basin, Argentina. A reassessment of age and carbon isotope stratigraphy. J Geol 124:171–193

Al-Suwaidi AH, Ruhl M, Jenkyns HC, Damborenea SE, Mancenido MO, Condon DJ, Angelozzi GN, Kamo SL, Storm M, Riccardi AC, Hesselbo SP (2022) New age constraints on the lower Jurassic Pliensbachian-Toarcian Boundary at Chacay Melehue (Neuquén Basin, Argentina). Sci Rep 12:4975

Baghli H, Mattioli E, Spangenberg JE, Ruebsam W, Schwark L, Bensalah M, Sebane A, Pittet B, Pellenard P, Suan G (2022) Stratification and productivity in the Western Tethys (NW Algeria) during early Toarcian. Palaeogeogr Palaeoclimatol Palaeoecol 59:1110864. https://doi.org/10.1016/j.palaeo.2022.110864

Bjerrum CJ, Surlyk F, Callomon JH, Slingerland RL (2001) Numerical paleoceanographic study of the early Jurassic transcontinental Laurasian Seaway. Paleoceanography 16:390–404

Blakey RC (2016) Global Jurassic Paleogeographic Map (180 Ma BP): Mollenweide Global Paleogeography and Tectonics in Deep Time

© 2016 Colorado Plateau Geosystems Inc. https://deeptimemaps.com

Bodin S, Mattioli E, Fröhlich S, Marshall JD, Boutib L, Lahsini S, Redfern J (2010) Toarcian carbon isotope shifts and nutrient changes from the northern margin of Gondwana (High Atlas, Marocco, Jurassic): palaeoenvironmental implications. Palaeogeogr Palaeoclimatol Palaeoecol 297:377–390

Bodin S, Fantasia A, Krencker FN, Nebsjerg B, Christiansen L, Andrieu S (2023) More gaps than record! A new look at the Pliensbachian/Toarcian boundary event guided by coupled chemosequence stratigraphy. Palaeogeogr Palaeoclimatol Palaeoecol 610:111344

Cohen AS, Coe AL, Harding SM, Schwark L (2004) Osmium isotope evidence for the regulation of atmospheric CO_2 by continental weathering. Geology 32:157–160

Danise S, Clémence ME, Price GD, Murphy DP, Gómez JJ, Twitchett RJ (2019) Stratigraphic and environmental control on marine benthic community change through the early Toarcian extinction event (Iberian Range, Spain). Palaeogeogr Palaeoclimatol Palaeoecol 524:183–200

Dera G, Donnadieu Y (2012) Modeling evidences for global warming, Arctic seawater freshening, and sluggish oceanic circulation during the early Toarcian anoxic event. Paleoceanography 27:PA2211

Dera G, Pellenard P, Neige P, Deconinck JF, Pucéat E, Dommergues JL (2009) Distribution of clay minerals in Early Jurassic Peritethyan seas: palaeoclimatic significance inferred from multiproxy comparisons. Palaeogeogr Palaeoclimatol Palaeoecol 271:39–51

Dera G, Brigaud B, Monna F, Laffont R, Pucéat E, Deconinck JF, Pellenard P, Joachimski MM, Durlet C (2011) Climatic ups and downs in a disturbed Jurassic world. Geology 39:215–218. https://doi.org/10.1130/G31579.1

Dickson AJ, Gill BC, Ruhl M, Jenkyns HC, Porcelli D, Idez E, Lyons TW, van den Boorn SHJM (2017) Molybdenum-isotope chemostratigraphy and paleoceanography of the Toarcian Oceanic Anoxic Event (Early Jurassic). Paleoceanography 32:813–829

Erba E, Cavalheiro L, Dickson AJ, Faucher G, Gambacorta G, Jenkyns HC, Wagner T (2022) Carbon- and oxygen-isotope signature of the Toarcian Oceanic Anoxic Event: insights from two Tethyan pelagic sequences (Gajum and Sogno Cores—Lombardy Basin, northern Italy). Newsl Stratigr 55:451–477

Fantasia A, Föllmi KB, Adatte T, Bernádez E, Spangenberg JE, Mattioli E (2018) The Toarcian Oceanic Anoxic Event in southwestern Gondwana: an example from the Andean Basin, northern Chile. J Geol Soc 175:883–902

Fantasia A, Adatte T, Spangenberg JE, Font E, Duarte LV, Föllmi KB (2019a) Global versus local processes during the Pliensbachian-Toarcian transition at the Peniche GSSP, Portugal: a multi-proxy record. Earth Sci Rev 198:102932

Fantasia A, Föllmi KB, Adatte T, Spangenberg JE, Mattioli E (2019b) Expresion of the Toarcian Oceanic Anoxic Event: new insights from a Swiss transect. Sedimentology 66:262–284

Fernández-Martínez J, Ruíz FM, Rodríguez-Tovar FJ, Piñuela L, García-Ramos JC, Algeo TJ (2023) Euxinia and hydrographic restriction in the Tethys Ocean: reassessing global oceanic anoxia during the early Toarcian. Global Planet Change 221:104026

Fu X, Wang J, Zeng S, Feng X, Wang D, Song C (2017) Continental weathering and palaeoclimatic changes through the onset ft he Early Toarcian oceanic anoxic event in the Qiangtang Basin, eastern Tethys. Palaeogeogr Palaeoclimatol Palaeoecol 487:241–250

Fu X, Wang J, Wen H, Song C, Wang Z, Zeng S, Feng X, Wei H (2021) A Toarcian Ocean Anoxic Event record from an open-ocean setting in the eastern Tethys: implications for global climatic change and regional environmental perturbation. Sci China Earth Sci 64:1860–1872

Galasso F, Feist-Burkardt S, Schneebeli-Herrmann E (2022) The palynology of the Toarcian Oceanic Anoxic Event at Dormettingen, southwest Germany, with emphasis on changes in vegetational dynamics. Rev Palaeobot Palynol 304:104701

Hammer O, Harper DAT, Ryan PD (2001) PAST: paleontological statistics software package for education and data analysis. Palaeontol Electron 4:1–9

Han Z, Hu X, Hu Z, Jenkyns HC, Su T (2022) Geochemical evidence from the Kioto Carbonate Platform (Tibet) reveals enhanced terrigenous input and deoxygenation during the early Toarcian. Global Planet Change 215:103887

Haq BU (2018) Jurassic sea level variations: a reappraisal. GSA Today 28:4–10

Hermoso M, Minoletti F, Pellenard P (2013) Black shale deposition during Toarcian super-greenhouse driven by sea level. Clim past 9:2703–2712

Hesselbo SP, Gröcke DR, Jenkyns HC, Bjerrum CJ, Farrimond P, Morgens Bell HS, Green OR (2000) Massive dissociation of gas hydrate during the Jurassic oceanic anoxic event. Nature 406:392–395

Hesselbo SP, Jenkyns HC, Duarte L, Oliveira LCV (2007) Carbon-isotope record of the Early Jurassic (Toarcian) Oceanic Anoxic Event from fossil wood and marine carbonate (Lusitanian Basin, Portugal). Earth Planet Sci Lett 253:455–470

Huang C, Hesselbo SP (2014) Pacing of the Toarcian Oceanic Anoxic Event (Early Jurassic) from astronomical correlation of marine sections. Gondwana Res 25:1348–1356

Huang Y, Jin X, Pancost RD, Kemp DB, Naafs DA (2023) An intensified lacustrine methane cycle during the Toarcian Oceanic Anoxic Event in the Ordos Basin. Pre-print, Research Square, 2023. https://doi.org/10.21203/rs.3.rs-2624197/v1

Hougård IW, Bojesen-Koefoed JA, Vickers ML, Ullmann CV, Bjerrum CJ, Rizzi M, Korte C (2021) Redox element record shows that environmental perturbations associated with the T-OAE were of longer duration than the carbon isotope record suggests—the Aubach section, SW Germany. Newsl Stratigr 54:229–246

Huang Y, Jin X, Pancost R, Kemp DB, Naafs B (2023) Intensification of the lacustrine methane cycle during the Toarcian Oceanic Anoxic Event. Preprint from Research Square, 07 Mar 2023, 1021203/rs3rs-2624197/v1 PPR: PPR626709

Izumi K, Kemp DB, Itamiya S, Inui M (2018) Sedimentary evidence for enhanced hydrological cycling in response to rapid carbon release during the early Toarcian oceanic anoxic event. Earth Planet Sci Lett 481:162–170

Jenkyns HC (1988) The early Toarcian (Jurassic) Anoxic Event: Stratigraphic, sedimentary, and geochemical evidence. Am J Sci 288:101–151

Jenkyns HC (2010) Geochemistry of oceanic anoxic events. Geochem Geophys Geosyst 11:1–30

Jenkyns HC, Clayton CJ (1986) Black shales and carbon isotopes in pelagic sediments from the Tethyan Lower Jurassic. Sedimentology 33:87–106

Jenkyns HC, Gröcke DR, Hesselbo SP (2001) Nitrogen isotope evidence for water mass denitrification during the early Toarcian (Jurassic) oceanic anoxic event. Paleoceanography 16:593–603

Jin X, Shi Z, Baranyi V, Kemp DB, Han Z, Luo G, Hu J, Chen L, Preto N (2020) The Jenkyns Event (early Toarcian OAE) in the Ordos Basin, North China. Global Planet Change 193:103273

Keeling RF, Körtzinger A, Gruber N (2010) Ocean deoxygenation in a warming world. Annu Rev Mar Sci 2:199–229

Kemp DB, Coe AL, Cohen AS, Schwark L (2005) Astronomical pacing of methane release in the Early Jurassic. Nature 437:396–399

Kemp DB, Chen W, Cho T, Algeo TJ, Shen J, Ikeda M (2022a) Deep-ocean anoxia across the Pliensbachian-Toarcian boundary and the Toarcian Oceanic Anoxic Event in the Panthalassic Ocean. Global Planet Change 212:103782

Kemp DB, Suan G, Fantasia A, Jin S, Chen W (2022b) Global organic carbon burial during the Toarcian oceanic anoxic event: pattern and controls. Earth Sci Rev 231:104086

Krencker FN, Lindström S, Bodin S (2019) A major sea-level drop briefly precedes the Toarcian oceanic anoxic event: implication for Early Jurassic climate and carbon cycle. Sci Rep 9:12518

Krencker FN, Fantasia A, El Ouali M, Kibiri L, Bodin S (2022) The effects of strong sediment-supply variability on the sequence stratigraphic architecture: insights from early Toarcian carbonate factory collapse. Mar Pet Geol 136:105469

Li B, Jin X, Dal Corso J, Ogg JG, Lang X, Baranyi V, Preto N, Franceschi M, Qiao P, Shi Z (2023) Complex pattern of environmental changes and organic matter preservation in the NE Ordos lacustrine depositional system (China) during the T-OAE (Early Jurassic). Global Planet Change 221:104045

Littke R, Baker DR, Leythaeuser D, Rullkötter J (1991a) Keys to the depositional history of the Posidonia Shale (Toarcian) in the Hils Syncline, northern Germany. In: Tyson RV, Pearson TH (eds) Modern and ancient continental shelf anoxia, vol 58. Geological Society, London, pp 311–333

Littke R, Rotzal H, Leythaeuser D, Baker DR (1991b) Lower Toarcian Posidonia Shale in Southern Germany (Schaebische Alb) Organofacies, depositional environment, and maturity. Erdoel Und Kohle Erdgas Petrochemie 44:407–414

Liu M, Sun P, Them TR, Li Y, Sun S, Gao X, Huang X, Tang Y (2020) Organic geochemistry of a lacustrine shale across the Toarcian Oceanic Anoxic Event (Early Jurassic) from NE China. Global Planet Change 191:103214

McArthur JM, Donovan DT, Thirlwall MF, Fouke BW, Mattey D (2000) Strontium isotope profile of the early Toarcian (Jurassic) oceanic anoxic event, the duration of ammonite biozones, and belemnite palaeotemperatures. Earth Planet Sci Lett 179:269–285

McArthur JM, Algeo TJ, van de Schootbrugge B, Li Q, Howarth RJ (2008) Basinal restriction, black shales, Re-Os dating, and the early Toarcian (Jurassic) oceanic anoxic event. Paleoceanography 23:PA4217

McElwain JC, Wade Murphy J, Hesselbo SP (2005) Changes in carbon dioxide during an anoxic event linked to intrusion of Gondwana coals. Nature 435:479–482

Müller T, Price GD, Bajnai D, Nyerges A, Kesjár D, Raucsik B, Varga A, Judi K, Fekete J, May Z, Pálfy J (2017) New multiproxy record of the Jenkyns Event (also known as the Toarcian Oceanic Anoxic Event) from the Mecsek Mountains (Hungary): differences, duration and drivers. Sedimentology 64:66–86

Nordt L, Breecker D, White J (2022) Jurassic greenhouse ice-sheet fluctuations sensitive to atmospheric CO_2 dynamics. Nat Geosci 15:54–59

Parrish JT, Curtis R (1982) Atmospheric circulation, upwelling, and organic-rich rocks in the Mesozoic and Cenozoic Eras Palaeogeography. Palaeoclimatol Palaeoecol 40:31–66

Percival LME, Cohen AS, Davies MK, Dickson AJ, Hesselbo SP, Jenkyns HC, Leng MJ, Mather TA, Storm M, Xu W (2016) Osmium isotope evidence for two pulses of increased continental weathering linked to early Jurassic volcanism and climate change. Geology 44:759–762

Pienkowski G, Hodbod M, Ullmann CV (2016) Fungal decomposition of terrestrial organic matter accelerated Early Jurassic climate warming. Sci Rep 6:31930

Pittet B, Suan G, Lenoir F, Duarte LV, Mattioli E (2014) Carbon isotope evidence for sedimentary discontinuities in the lower Toarcian of the Lusitanian Basin (Portugal): sea level change at the onset of the Oceanic Anoxic Event. Sed Geol 303:1–14

Prauss M (1996) The Lower Toarcian Posidonia Shale of Grimmen, Northeast Germany. Implications from the palynological analysis of a near-shore section. N Jb Geol Paläont 200:107–132

Rees PM, Ziegler AM, Valdes PJ (2000) Jurassic phytogeography and climates: new data and model comparisons. In: Huber BT, Macleod KG, Wing SL (eds) Warm climates in Earth history. Cambridge University Press, Cambridge, pp 297–318

Remírez MN, Algeo TJ (2020) Paleosalinity determination in ancient epicontinental seas: a case study of the T-OAE in the Cleveland Basin (UK). Earth Sci Rev 201:103072

Reolid M, Molina JM, Nieto LM, Rodríguez-Tovar FJ (2018) The Toarcian oceanic anoxic event in the South Iberian Palaeomargin. Springer Briefs in Earth Sciences, Cham, p 122

Reolid M, Mattioli E, Duarte LV, Ruebsam W (2021) The early Toarcian Oceanic Anoxic Event: where do we stand? In: Reolid M, Mattioli E, Duarte LV, Ruebsam W (eds) Carbon cycle and ecosystem response to the Jenkyns Event in the Early Toarcian (Jurassic), vol 514. GSL Special Publications. 101144/SP514-2021-74

Röhl HJ, Schmid-Röhl A, Oschmann W, Frimmel A, Schwark L (2001) The Posidonia Shale (lower Toarcian) of SW-Germany: an oxygen-depleted ecosystem controlled by sea level and palaeoclimate. Palaeogeogr Palaeoclimatol Palaeoecol 165:27–52

Ruebsam W, Al-Husseini M (2020) Calibrating the early Toarcian (early Jurassic) with stratigraphic black holes (SBH). Gondwana Res 82:317–336

Ruebsam W, Müller T, Kovács J, Pálfy J, Schwark L (2018) Environmental response to the early Toarcian carbon cycle and climate perturbations in the northeastern part of the West-Tethys shelf. Gondwana Res 59:144–158

Ruebsam W, Mayer B, Schwark L (2019) Cryosphere carbon dynamics control early Toarcian global warming and sea level evolution. Global Planet Change 172:440–453

Ruebsam W, Reolid M, Sabatino N, Masetti D, Schwark L (2020a) Molecular paleothermometry of the early Toarcian climate perturbation. Global Planet Change 195:103351

Ruebsam W, Thibault N, Al-Husseini M (2020b) Chapter 12—early Toarcian glacioeustatic unconformities and chemostratigraphic black holes. In: Montenari M (ed) Stratigraphy and timescales, vol 5, Carbon Isotope Stratigraphy. https://doi.org/10.1016/bs.sats.2020.08.006

Ruebsam W, Reolid M, Schwark L (2020c) $\delta^{13}C$ of terrestrial vegetation records Toarcian CO_2 and climate gradients. Nat Sci Rep 10:117. https://doi.org/10.1038/s41598-019-56710-6

Ruebsam W, Reolid M, Marok A, Schwark L (2020d) Drivers of benthic extinction during the early Toarcian (Early Jurassic) at the northern Gondwana paleomargin: implications for paleoceanographic conditions. Earth Sci Rev 203:103117. https://doi.org/10.1016/j.earscirev.2020.103117

Ruebsam W, Mattioli E, Schwark L (2022a) Weakening of the biological pump induced by a biocalcification crisis during the early Toarcian Oceanic Anoxic Event. Global Planet Change 217:103954

Ruebsam W, Reolid M, Mattioli E, Schwark L (2022b) Organic carbon accumulation at the northern Gondwana paleo-margin (Tunisia) during the Toarcian Oceanic Anoxic Event: Sedimentological and geochemical evidence. Palaeogeogr Palaeoclimatol Palaeoecol 586:110781

Ruebsam W, Schmid-Röhl A, Al-Husseini M (2023) Astronomical timescale for the early Toarcian (Early Jurassic) Posidonia Shale and global environmental changes. Palaeogeogr Palaeoclimatol Palaeoecol 623:111619

Ruvalcaba Baroni I, Pohl A, van Helmond NAGM, Papadomanolaki NM, Coe AL, Cohen AS et al (2018) Ocean circulation in the Toarcian (early Jurassic): a key control on deoxygenation and carbon burial on the European shelf. Paleoceanogr Paleoclimatol 33:994–1012

Sælen G, Doyle P, Talbot MR (1996) Stable-isotope analysis of belemnite rosta from the Whitby Mudstone Fm, England: surface water conditions during deposition of a marine black shale. Palaios 11:97–117

Sarmiento JL, Hughes TMC, Stouffer RJ, Manabe S (1998) Simulated response of the ocean carbon cycle to anthropogenic climate warming. Nature 393:245–249

Schlanger SO, Jenkyns HC (1976) Cretaceous oceanic anoxic events: causes and consequences. Geol Mijnbouw 55:179–184

Schouten S, van Kaam-Peters HME, Rijpstra WIC, Schoell M, Sinninghe Damsté JS (2000) Effects of an Oceanic Anoxic Event on the stable carbon isotopic composition of early Toarcian carbon. Am J Sci 300:1–22

Schwark L, Frimmel A (2004) Chemostratigraphy of the Posidonia Black Shale, SW-Germany: II assessment of extent and persistence of photic-zone anoxia using aryl isoprenoid distributions. Chem Geol 206:231–248

Silva R, Ruhl M, Barry C, Reolid M, Ruebsam W (2021) Pacing of Late Pliensbachian and Early Toarcian carbon cycle perturbations and environmental change in the westernmost Tethys (La Cerradura section, Subbetic Zone of the Betic Cordillera, Spain). In: Reolid M, Mattioli E, Duarte LV, Ruebsam W (eds) Carbon Cycle and Ecosystem Response to the Jenkyns Event in the Early Toarcian (Jurassic), vol 514. GSL Special Publications. https://doi.org/10.1144/SP514-2021-27

Song J, Littke R, Weniger P (2017) Organic geochemistry of the lower Toarcian Posidonia Shale in NW Europe. Org Geochem 106:76–92

Suan G, Nikitenko BL, Rogov MA, Baudin F, Spangenberg JE, Knyazev VG, Glinskikh LA, Goryacheva AA, Adatte T, Riding JB, Föllmi KB, Pittet B, Mattioli E, Lécuyer C (2011) Polar record of Early Jurassic massive carbon injection. Earth Planet Sci Lett 312:102–113

Sundararaman P, Schoell M, Littke R, Leythaeuser D, Rullkötter J (1993) Depositional environment of Toarcian shales from northern Germany as monitored with porphyrins. Geochim Cosmochim Acta 57:4213–4218

Them TR, Gill BC, Selby D, Gröcke DR, Friedman RM, Owens JD (2017) Evidence for rapid weathering response to climatic warming during the Toarcian Oceanic Anoxic Event. Sci Rep 7:5003

Them TR, Gill BC, Caruthers AH, Gerhardt AM, Gröcke DR, Lyons TW, Marroquin SM, Nielsen SG, Trabucho Alexandre JP, Owens JD (2018) Thallium isotopes reveal protracted anoxia during the Toarcian (Early Jurassic) associated with volcanism, carbon burial, and mass extinction. Proc Natl Acad Sci 115:6596–6601

Thibault N, Ruhl M, Ullmann CV, Korte C, Kemp DB, Gröcke DR, Hesselbo SP (2018) The wider context of the lower Jurassic Toarcian oceanic anoxic event in Yorkshire coastal outcrops, UK. Proc Geol Assoc 129:372–391

Trabucho-Alexandre JP, Gröcke DR, Atar E, Herringshaw L, Jarvis I (2022) A new subsurface record of the Pliensbachian–Toarcian, Lower Jurassic, of Yorkshire. Proc Yorks Geol Soc 64. https://doi.org/10.1144/pygs2022-007

Tyson RV, Pearson TH (1991) Modern and ancient continental shelf anoxia: an overview. Geol Soc Lond Spec Publ 58:1–24

Visentin S, Erba E, Mutterlose J (2021) Bio- and chemostratigraphy of the Posidonia Shale: a new database for the Toarcian Oceanic Anoxic Event from northern Germany. Newsl Stratigr 55:173–198

Wignall PB (1991) Model for transgressive black shales? Geology 19:167–170

Wignall PB (1994) Black shales. Oxford University Press, Oxford, p 127

Xia G, Mansour A (2022) Paleoenvironmental changes during the early Toarcian Oceanic Anoxic Event: insights into organic carbon distribution and controlling mechanisms in the eastern Tethys. J Asian Earth Sci 237:105344

Xu W, Ruhl M, Jenkyns HC, Hesselbo SP, Riding JB, Selby D, Naafs BDA, Weijers JWH, Pancost RD, Tegelaar EW, Idez EF (2017) Carbon sequestration in an expanded lake system during the Toarcian oceanic anoxic event. Nat Geosci 10:129–134